

# Supplementary Materials for “Personalized Biopsies in Prostate Cancer Active Surveillance”

Anirudh Tomer, MSc<sup>a,\*</sup>, Dimitris Rizopoulos, PhD<sup>a</sup>, Daan Nieboer, MSc<sup>b</sup>,  
Monique J. Roobol, PhD<sup>c</sup>, Au Thor<sup>d</sup>, Aut Hor<sup>d</sup>, Auth Or<sup>d</sup>

<sup>a</sup>*Department of Biostatistics, Erasmus University Medical Center, Rotterdam, the Netherlands*

<sup>b</sup>*Department of Public Health, Erasmus University Medical Center, Rotterdam, the Netherlands*

<sup>c</sup>*Department of Urology, Erasmus University Medical Center, Rotterdam, the Netherlands*

<sup>d</sup>*Department of xxxx, xxxx University Medical Center, City, Country*

---

---

## Appendix A. A Joint Model for the Longitudinal PSA, and Time to Gleason $\geq 7$

### Appendix A.1. Study Cohort

Prostate Cancer International Active Surveillance (PRIAS) is an ongoing prospective cohort study of men with low- and very-low risk PCa diagnoses [1]. More than 100 medical centers from 17 countries contribute in PRIAS, using a common study protocol ([www.prias-project.org](http://www.prias-project.org)). We used the data collected between December 2006 (beginning of PRIAS study) and May 2019. The PSA was measured every three months until year two of follow-up and every six months thereafter. Biopsy schedule was year one, four, seven, and ten, and additional yearly biopsies when PSA doubling time is between zero and ten years. The primary event of this work is Gleason  $\geq 7$  (GS7). It was observed in 1134 patients, but 2250 were provided treatment (see Table 1). Treatment in absence of GS7 may have been advised on the basis of PSA, number of biopsy cores with cancer, anxiety, or other reasons.

---

\*Corresponding author (Anirudh Tomer): Erasmus MC, kamer flex Na-2823, PO Box 2040, 3000 CA Rotterdam, the Netherlands. Tel: +31 10 70 43393

Email addresses: [a.tomer@erasmusmc.nl](mailto:a.tomer@erasmusmc.nl) (Anirudh Tomer, MSc),  
[d.rizopoulos@erasmusmc.nl](mailto:d.rizopoulos@erasmusmc.nl) (Dimitris Rizopoulos, PhD), [d.nieboer@erasmusmc.nl](mailto:d.nieboer@erasmusmc.nl)  
(Daan Nieboer, MSc), [m.roobol@erasmusmc.nl](mailto:m.roobol@erasmusmc.nl) (Monique J. Roobol, PhD)

16 We focused only on GS7 because of its strong association with cancer-related  
 17 outcomes. Due to the periodical nature of biopsies, the time of GS7 was only  
 18 known as a time interval in which it occurred.

Table 1: **Patient characteristics for the PRIAS dataset.** The primary event of interest is Gleason  $\geq 7$ . IQR: interquartile range, PSA: prostate-specific antigen.

Characteristic	Value
Total patients	7813
Gleason $\geq 7$ (primary event)	1134
Treatment	2250
Watchful waiting	334
Loss to follow-up	250
Death (unrelated to prostate cancer)	95
Death (related to prostate cancer)	2
Median age at diagnosis (years)	61 (IQR: 66–71)
Median follow-up period per patient (years)	1.8 (IQR: 0.9–3.99)
Total PSA measurements	65798
Median number of PSA measurements per patient	6 (IQR: 4–12)
Median PSA value (ng/mL)	5.7 (IQR: 4.1–7.7)
Total biopsies	15563
Median number of biopsies per patient	2 (IQR: 1–3)

## 19 Appendix A.2. Model Definition

20 Let  $T_i^*$  denote the true time of GS7 for the  $i$ -th patient included in PRIAS.  
 21 Since biopsies are conducted periodically,  $T_i^*$  is observed with interval cen-  
 22 soring  $l_i < T_i^* \leq r_i$ . When GS7 is observed for the patient at his latest biopsy  
 23 time  $r_i$ , then  $l_i$  denotes the time of the second latest biopsy. Otherwise,  $l_i$   
 24 denotes the time of the latest biopsy and  $r_i = \infty$ . Let  $\mathbf{y}_i$  denote his ob-  
 25 served PSA longitudinal measurements. The observed data of all  $n$  patients  
 26 is denoted by  $\mathcal{D}_n = \{l_i, r_i, \mathbf{y}_i; i = 1, \dots, n\}$ .

In our joint model, the patient-specific PSA measurements over time are modeled using a linear mixed effects sub-model. It is given by (see Panel A, Figure 1):

$$\log_2 \{y_i(t) + 1\} = m_i(t) + \varepsilon_i(t),$$

$$m_i(t) = \beta_0 + b_{0i} + \sum_{k=1}^4 (\beta_k + b_{ki}) B_k \left( \frac{t-2}{2}, \frac{\mathcal{K}-2}{2} \right) + \beta_5 \text{age}_i, \quad (1)$$

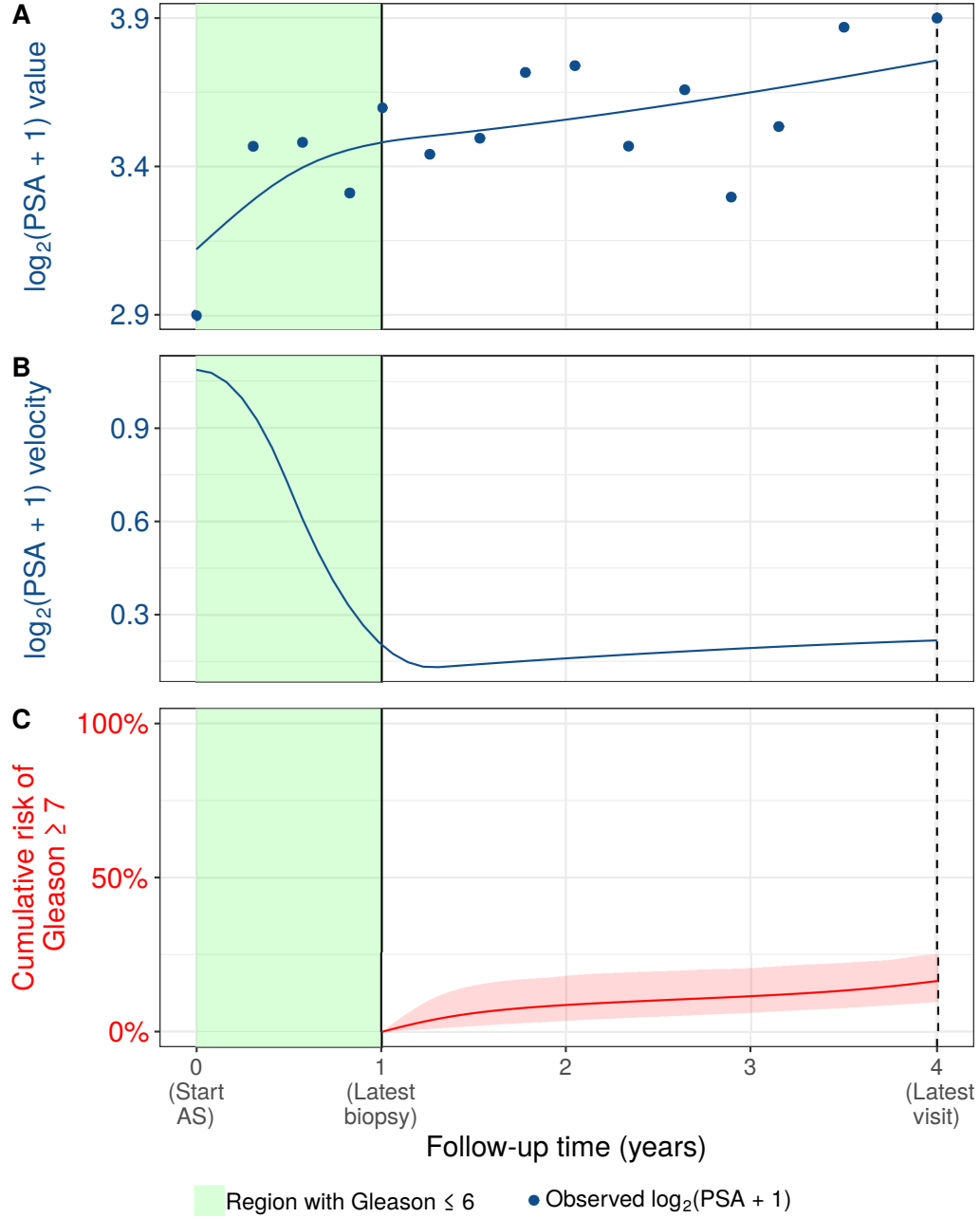


Figure 1: **Illustration of the joint model fitted to the PRIAS dataset.** **Panel A:** shows the observed and fitted  $\log_2(\text{PSA} + 1)$  measurements (Equation 1). **Panel B:** shows the estimated  $\log_2(\text{PSA} + 1)$  velocity over time, mathematically derived from Equation (1). The cumulative risk of Gleason  $\geq 7$  (Equation 2) shown in **Panel C**, depends on the fitted  $\log_2(\text{PSA} + 1)$  value and velocity, and the time of the latest biopsy (year 1 in this case).

where,  $m_i(t)$  denotes the measurement error free value of  $\log_2(\text{PSA} + 1)$  transformed [2, 3] measurements at time  $t$ . We model it non-linearly over time using B-splines [4]. To this end, our B-spline basis function  $B_k\{(t - 2)/2, (\mathcal{K} - 2)/2\}$  has 3 internal knots at  $\mathcal{K} = \{0.5, 1.3, 3\}$  years, which are the three quartiles of the observed follow-up times. The boundary knots of the spline are at 0 and 6.3 years (95-th percentile of the observed follow-up times). We mean centered (mean 2 years) and standardized (standard deviation 2 years) the follow-up time  $t$  and the knots of the B-spline  $\mathcal{K}$  during parameter estimation for better convergence. The fixed effect parameters are denoted by  $\{\beta_0, \dots, \beta_5\}$ , and  $\{b_{0i}, \dots, b_{4i}\}$  are the patient specific random effects. The random effects follow a multivariate normal distribution with mean zero and variance-covariance matrix  $\mathbf{D}$ . The error  $\varepsilon_i(t)$  is assumed to be t-distributed with three degrees of freedom (see Appendix B.1) and scale  $\sigma$ , and is independent of the random effects.

To model the impact of PSA measurements on the risk of GS7, our joint model uses a relative risk sub-model. More specifically, the hazard of GS7 denoted as  $h_i(t)$ , and the cumulative risk of GS7 denoted as  $R_i(t)$ , at a time  $t$  are (see Panel C, Figure 1):

$$\begin{aligned} h_i(t) &= h_0(t) \exp \left( \gamma \text{age}_i + \alpha_1 m_i(t) + \alpha_2 \frac{\partial m_i(t)}{\partial t} \right), \\ R_i(t) &= \exp \left\{ - \int_0^t h_i(s) ds \right\}, \end{aligned} \tag{2}$$

where,  $\gamma$  is the parameter for the effect of age. The impact of PSA on the hazard of GS7 is modeled in two ways, namely the impact of the error free underlying PSA value  $m_i(t)$  (see Panel A, Figure 1), and the impact of the underlying PSA velocity  $\partial m_i(t)/\partial t$  (see Panel B, Figure 1). The corresponding parameters are  $\alpha_1$  and  $\alpha_2$ , respectively. Lastly,  $h_0(t)$  is the baseline hazard at time  $t$ , and is modeled flexibly using P-splines [5]. More specifically:

$$\log h_0(t) = \gamma_{h_0,0} + \sum_{q=1}^Q \gamma_{h_0,q} B_q(t, \mathbf{v}),$$

where  $B_q(t, \mathbf{v})$  denotes the  $q$ -th basis function of a B-spline with knots  $\mathbf{v} = v_1, \dots, v_Q$  and vector of spline coefficients  $\gamma_{h_0}$ . To avoid choosing the number and position of knots in the spline, a relatively high number of knots (e.g., 15 to 20) are chosen and the corresponding B-spline regression coefficients  $\gamma_{h_0}$  are penalized using a differences penalty [5].

### 46 *Appendix A.3. Parameter Estimation*

We estimate the parameters of the joint model using Markov chain Monte Carlo (MCMC) methods under the Bayesian framework. Let  $\boldsymbol{\theta}$  denote the vector of all of the parameters of the joint model. The joint model postulates that given the random effects, the time of GS7, and the PSA measurements taken over time are all mutually independent. Under this assumption the posterior distribution of the parameters is given by:

$$\begin{aligned} p(\boldsymbol{\theta}, \mathbf{b} \mid \mathcal{D}_n) &\propto \prod_{i=1}^n p(l_i, r_i, \mathbf{y}_i \mid \mathbf{b}_i, \boldsymbol{\theta}) p(\mathbf{b}_i \mid \boldsymbol{\theta}) p(\boldsymbol{\theta}) \\ &\propto \prod_{i=1}^n p(l_i, r_i \mid \mathbf{b}_i, \boldsymbol{\theta}) p(\mathbf{y}_i \mid \mathbf{b}_i, \boldsymbol{\theta}) p(\mathbf{b}_i \mid \boldsymbol{\theta}) p(\boldsymbol{\theta}), \\ p(\mathbf{b}_i \mid \boldsymbol{\theta}) &= \frac{1}{\sqrt{(2\pi)^q \det(\mathbf{D})}} \exp(\mathbf{b}_i^T \mathbf{D}^{-1} \mathbf{b}_i), \end{aligned}$$

where, the likelihood contribution of the PSA outcome, conditional on the random effects is:

$$p(\mathbf{y}_i \mid \mathbf{b}_i, \boldsymbol{\theta}) = \frac{1}{(\sqrt{2\pi\sigma^2})^{n_i}} \exp\left(-\frac{\|\mathbf{y}_i - \mathbf{m}_i\|^2}{\sigma^2}\right),$$

The likelihood contribution of the time of GS7 outcome is given by:

$$p(l_i, r_i \mid \mathbf{b}_i, \boldsymbol{\theta}) = \exp\left\{-\int_0^{l_i} h_i(s) ds\right\} - \exp\left\{-\int_0^{r_i} h_i(s) ds\right\}. \quad (3)$$

47 The integral in (3) does not have a closed-form solution, and therefore we  
48 use a 15-point Gauss-Kronrod quadrature rule to approximate it.

49 We use independent normal priors with zero mean and variance 100 for  
50 the fixed effects  $\{\beta_0, \dots, \beta_5\}$ , and inverse Gamma prior with shape and rate  
51 both equal to 0.01 for the parameter  $\sigma^2$ . For the variance-covariance matrix  
52  $\mathbf{D}$  of the random effects we take inverse Wishart prior with an identity scale  
53 matrix and degrees of freedom equal to 5 (number of random effects). For  
54 the relative risk model's parameter  $\gamma$  and the association parameters  $\alpha_1, \alpha_2$ ,  
55 we use independent normal priors with zero mean and variance 100.

### 56 *Appendix A.4. Parameter Estimates*

57 The joint model was fitted using the R package **JMbayes** [6]. This pack-  
58 age utilizes the Bayesian methodology to estimate model parameters. The

corresponding posterior parameter estimates are shown in Table 3 (longitudinal sub-model for PSA outcome) and Table 4 (relative risk sub-model). The parameter estimates for the variance-covariance matrix  $\mathbf{D}$  from the longitudinal sub-model for PSA are shown in the following Table 2:

Table 2: Estimated variance-covariance matrix  $\mathbf{D}$  of the random effects  $\mathbf{b} = (b_0, b_1, b_2, b_3, b_4)$  (see Appendix A.2) from the joint model fitted to the PRIAS dataset. The variances of the random effects are highlighted along the diagonal of the variance-covariance matrix.

Random Effects	$b_0$	$b_1$	$b_2$	$b_3$	$b_4$
$b_0$	<b>0.229</b>	0.029	0.022	0.070	0.005
$b_1$	0.029	<b>0.149</b>	0.097	0.169	0.085
$b_2$	0.022	0.097	<b>0.270</b>	0.326	0.231
$b_3$	0.070	0.169	0.326	<b>0.550</b>	0.355
$b_4$	0.005	0.085	0.231	0.355	<b>0.348</b>

For the PSA mixed effects sub-model parameter estimates (see Equation 1), in Table 3 we can see that the age of the patient trivially affects the baseline  $\log_2(\text{PSA} + 1)$  measurement. Since the longitudinal evolution of  $\log_2(\text{PSA} + 1)$  measurements is modeled with non-linear terms, the interpretation of the coefficients corresponding to time is not straightforward. In lieu of the interpretation, in Figure 2 we present plots of observed versus fitted PSA profiles for nine randomly selected patients.

Table 3: Estimated mean and 95% credible interval for the parameters of the longitudinal sub-model (see Equation 1) for the PSA outcome.

Variable	Mean	Std. Dev	2.5%	97.5%	P
Intercept	2.124	0.054	2.024	2.236	<0.001
Age	0.009	0.001	0.007	0.010	<0.001
Spline: [0.0, 0.5] years	0.062	0.006	0.050	0.075	<0.001
Spline: [0.5, 1.3] years	0.194	0.011	0.175	0.214	<0.001
Spline: [1.3, 3.0] years	0.243	0.014	0.218	0.269	<0.001
Spline: [3.0, 6.3] years	0.382	0.014	0.356	0.408	<0.001
$\sigma$	0.139	0.001	0.137	0.140	

For the relative risk sub-model (see Equation 2), the parameter estimates in Table 4 show that  $\log_2(\text{PSA} + 1)$  velocity and age of the patient were significantly associated with the hazard of GS7.

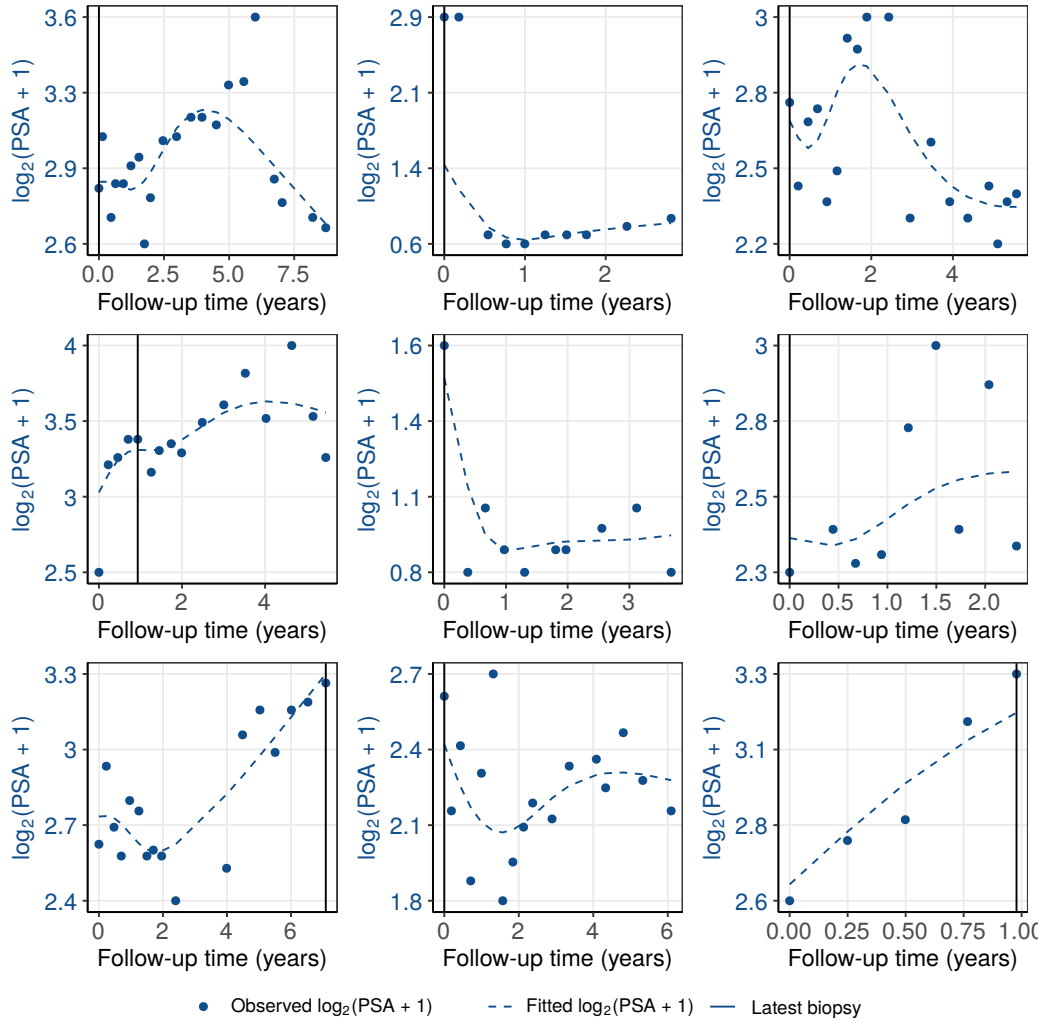


Figure 2: Fitted versus observed  $\log_2(\text{PSA} + 1)$  profiles for nine randomly selected PRIAS patients. The fitted profiles utilize information from the observed PSA measurements, and time of the latest biopsy.

Table 4: Estimated mean and 95% credible interval for the parameters of the relative risk sub-model (see Equation 2) of the joint model fitted to the PRIAS dataset.

Variable	Mean	Std. Dev	2.5%	97.5%	P
Age	0.037	0.006	0.026	0.049	<0.001
Fitted $\log_2(\text{PSA} + 1)$ value	-0.013	0.078	-0.157	0.143	0.812
Fitted $\log_2(\text{PSA} + 1)$ velocity	2.297	0.303	1.670	2.789	<0.001

It is important to note that since age, and  $\log_2(\text{PSA} + 1)$  value and velocity are all measured on different scales, a comparison between the corresponding parameter estimates is not easy. To this end, in Table 5, we present the hazard (of GS7) ratio, for an increase in the aforementioned variables from their first to the third quartile. For example, an increase in fitted  $\log_2(\text{PSA} + 1)$  velocity from -0.086 to 0.307 (fitted first and third quartiles) corresponds to a hazard ratio of 2.466. The interpretation for the rest is similar.

Table 5: Hazard (of GS7) ratio and 95% credible interval (CI), for an increase in the variables of relative risk sub-model, from their first quartile ( $Q_1$ ) to their third quartile ( $Q_3$ ). Except for age, quartiles for all other variables are based on their fitted values obtained from the joint model fitted to the PRIAS dataset.

Variable	$Q_1$	$Q_3$	Hazard ratio [95% CI]
Age	61	71	1.452 [1.298, 1.631]
Fitted $\log_2(\text{PSA} + 1)$ value	2.359	3.074	0.991 [0.894, 1.108]
Fitted $\log_2(\text{PSA} + 1)$ velocity	-0.086	0.307	2.466 [1.927, 2.992]

#### Appendix A.5. Assumption of $t$ -distributed ( $df=3$ ) Error Terms

With regards to the choice of the distribution for the error term  $\varepsilon$  for the PSA measurements (see Equation 1), we attempted fitting multiple joint models differing in error distribution, namely  $t$ -distribution with three, and four degrees of freedom, and a normal distribution for the error term. However, the model assumption for the error term were best met by the model with  $t$ -distribution having three degrees of freedom. The quantile-quantile plot of subject-specific residuals for the corresponding model in Panel A of Figure 3, shows that the assumption of  $t$ -distributed ( $df=3$ ) errors is reasonably met by the fitted model.



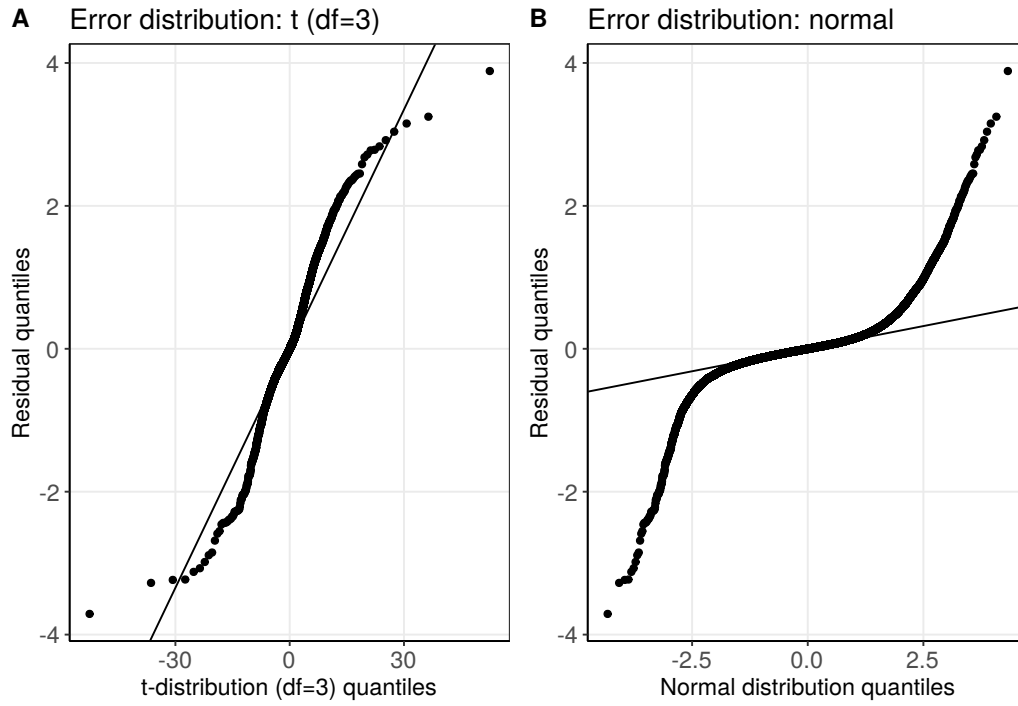


Figure 3: Quantile-quantile plot of subject-specific residuals from the joint models fitted to the PRIAS dataset. **Panel A:** model assuming a t-distribution ( $df=3$ ) for the error term  $\varepsilon$  (see Equation 1). **Panel B:** model assuming a normal distribution for the error term  $\varepsilon$ .

## 91 Appendix B. Obtaining Dynamic Risk Predictions from the Joint 92 Model

Let us assume a new patient  $j$ , for whom we need to estimate the risk of GS7. Let his current follow-up visit time be  $s$ , latest time of biopsy be  $t$ , observed vector PSA measurements be  $\mathcal{Y}_j(s)$ . The combined information from the observed data about the time of GS7, is given by the following posterior predictive distribution  $g(T_j^*)$  of his time  $T_j^*$  of GS7:

$$\begin{aligned} g(T_j^*) &= p\{T_j^* \mid T_j^* > t, \mathcal{Y}_j(s), \mathcal{D}_n\} \\ &= \int \int p(T_j^* \mid T_j^* > t, \mathbf{b}_j, \boldsymbol{\theta}) \\ &\quad \times p\{\mathbf{b}_j \mid T_j^* > t, \mathcal{Y}_j(s), \boldsymbol{\theta}\} p(\boldsymbol{\theta} \mid \mathcal{D}_n) d\mathbf{b}_j d\boldsymbol{\theta}. \end{aligned}$$

93 The distribution  $g(T_j^*)$  depends not only depends on the observed data of the  
94 patient  $T_j^* > t, \mathcal{Y}_j(s)$ , but also depends on the information from the PRIAS  
95 dataset  $\mathcal{D}_n$ . To this the the posterior distribution of random effects  $\mathbf{b}_j$  and  
96 posterior distribution of the vector of all parameters  $\boldsymbol{\theta}$  are utilized, respec-  
97 tively. The distribution  $g(T_j^*)$  can be estimated as detailed in Rizopoulos  
98 et al. [7]. Since, majority of the prostate cancer patients do not obtain GS7  
99 in the ten year follow-up period of PRIAS,  $g(T_j^*)$  can only be estimated for  
100 time points falling within the ten year follow-up.

The cumulative risk of GS7 can be derived from  $g(T_j^*)$  as given in [7]. It is given by:

$$R_j(u \mid t, s) = \Pr\{T_j^* > u \mid T_j^* > t, \mathcal{Y}_j(s), \mathcal{D}_n\}, \quad u \geq t. \quad (4)$$

101 The personalized risk profile of the patient (see Panel C, Figure 4) updates  
102 as more data is gathered over follow-up visits.

### 103 Appendix B.1. Validation of Risk Predictions

104 We validated the predictions of GS7 internally within the PRIAS dataset,  
105 as well as externally in five AS cohorts from the GAP3 database, having  
106 the longest follow-up periods [8]. These are the University of Toronto AS  
107 (Toronto), Johns Hopkins AS (JHAS), Memorial Sloan Kettering Cancer  
108 Center AS (MSKCC), King's College London Active Surveillance (KCL),  
109 and .... In all of these cohorts, we calculated the area under the receiver  
110 operating characteristic curve or AUC [7] as a measure of discrimination  
111 between patients who obtain GS7 and those do not obtain GS7. We also

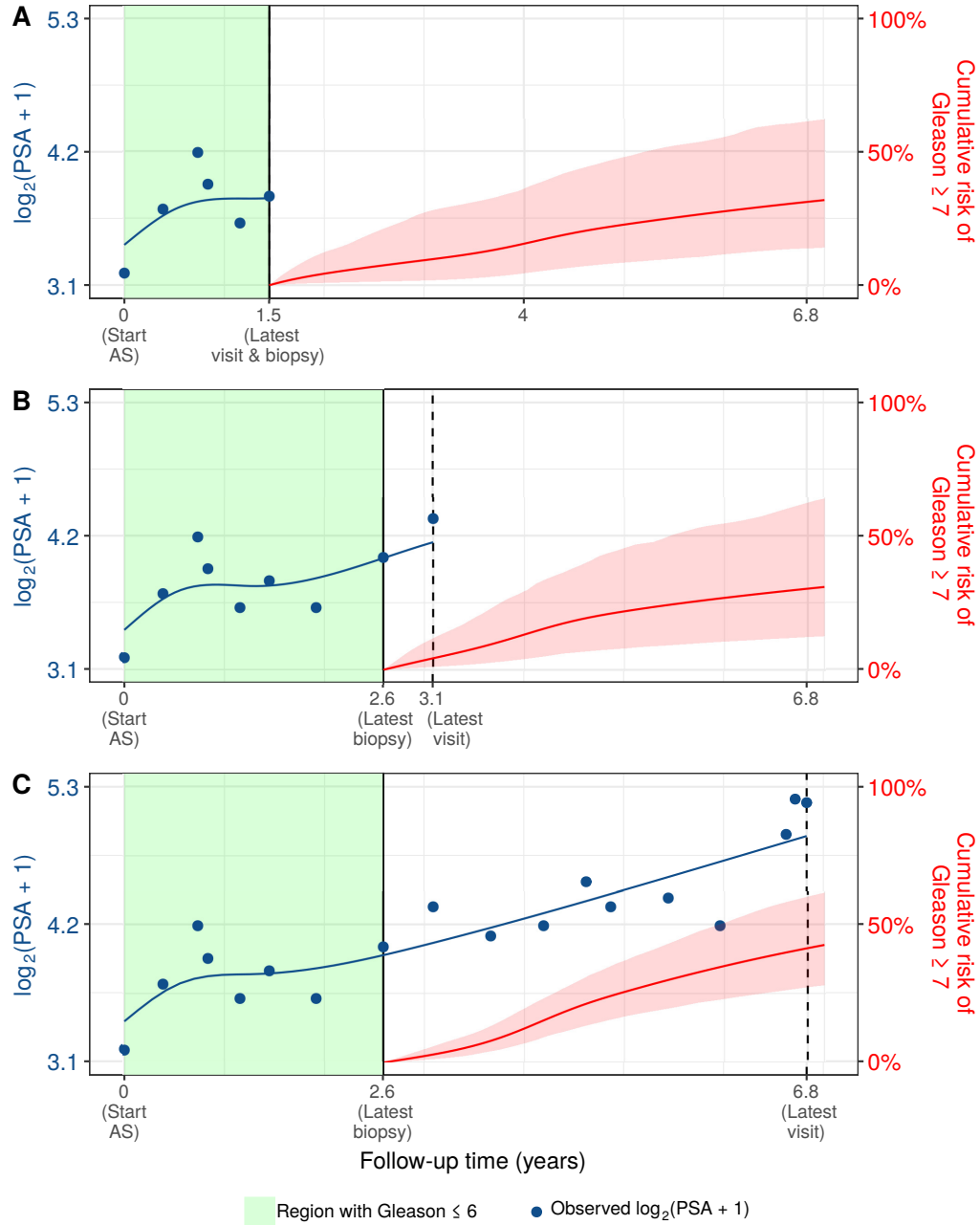


Figure 4: **Cumulative risk of Gleason  $\geq 7$  (GS7) changing dynamically over follow-up** as more patient data is gathered. The three **Panels A,B and C:** are ordered by the time of the latest visit (dashed vertical black line) of a new patient. At each of the latest follow-up visits, we combine the information from observed PSA measurements (shown in blue), and latest time of negative biopsy (solid vertical black line) to obtain the updated cumulative risk profile (shown in red) of the patient.

calculated root mean squared prediction error or RMSPE [7] as a measure of calibration. Both AUC and RMSPE take a value between 0 and 1. Ideally RMSPE should be 0 and AUC should 1. In addition, it is preferred that  $AUC > 0.5$  because an  $AUC \leq 0.5$  indicates that the model performs worse than random discrimination. Since AS studies are longitudinal in nature, AUC and RMSPE are also time dependent. More specifically, given the time of latest biopsy  $t$ , and history of PSA measurements up to time  $s$ , we calculate AUC and RMSPE for a medically relevant time frame  $(t, s]$ , within which the occurrence of GS7 is of interest. In the case of prostate cancer, at any point in time  $s$  it is of interest to identify patients who may have obtained GS7 in the last one year  $(s - 1, s]$ . That is we set  $t = s - 1$ . We then calculate AUC and RMSPE at a gap of every six months (follow-up schedule of PRIAS) until year five (95-percentile of the observed times of GS7), that is,  $s \in \{1, 1.5, \dots, 5\}$  years. The resulting estimates are summarized in Figure 5, and in Table 6 to Table 10.

Table 6: **Internal Validation of predictions of Gleason  $\geq 7$  (GS7) in PRIAS cohort.** The area under the receiver operating characteristic curve or AUC (measure of discrimination) root mean squared prediction error or RMSPE (measure of calibration) are calculated over the follow-up period at a gap of 6 months. In addition bootstrapped 95% confidence intervals (CI) are also presented.

Follow-up period (years)	AUC (95% CI)	RMSPE (95%CI)
0.0 to 1.0	0.656 [0.623, 0.690]	0.227 [0.223, 0.236]
0.5 to 1.5	0.657 [0.641, 0.671]	0.376 [0.371, 0.382]
1.0 to 2.0	0.663 [0.651, 0.678]	0.371 [0.364, 0.379]
1.5 to 2.5	0.650 [0.600, 0.684]	0.253 [0.245, 0.263]
2.0 to 3.0	0.676 [0.641, 0.725]	0.252 [0.241, 0.262]
2.5 to 3.5	0.689 [0.629, 0.732]	0.238 [0.224, 0.251]
3.0 to 4.0	0.652 [0.614, 0.709]	0.273 [0.263, 0.285]
3.5 to 4.5	0.625 [0.591, 0.663]	0.338 [0.326, 0.349]
4.0 to 5.0	0.623 [0.587, 0.657]	0.338 [0.325, 0.350]

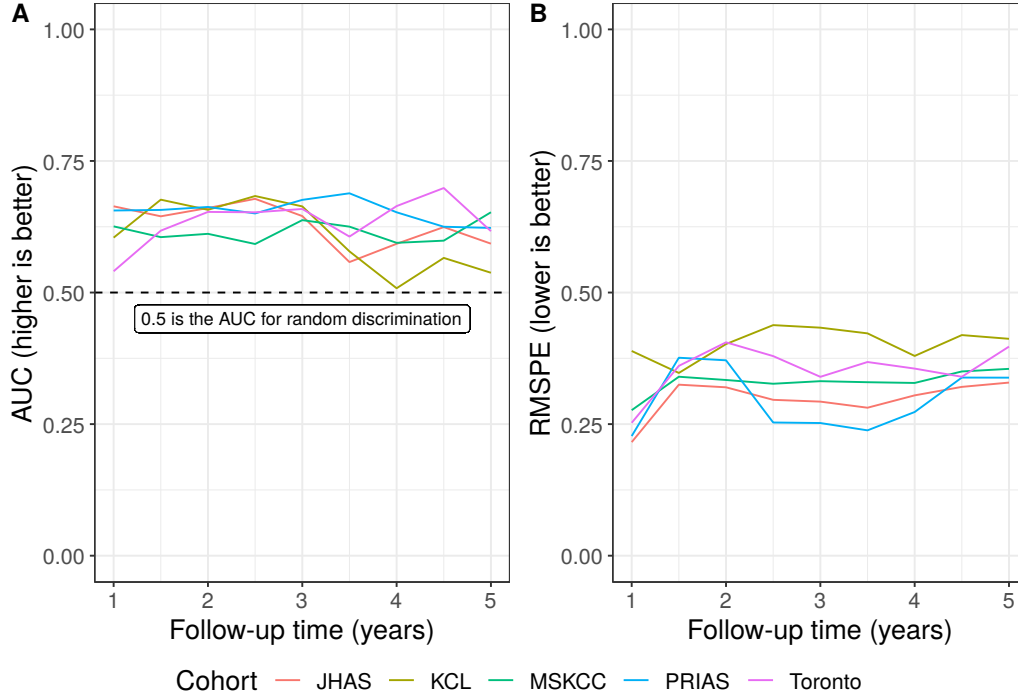


Figure 5: **Validation of predictions of Gleason  $\geq 7$  (GS7).** In **Panel A** we can see that the time dependent area under the receiver operating characteristic curve or AUC (measure of discrimination) is above 0.5 in PRIAS (internal validation), and JHAS and Toronto cohorts (external validation). In **Panel B** we can see that the time dependent root mean squared prediction error or RMSPE (measure of calibration) is similar for PRIAS, and JHAS and Toronto cohorts. The bootstrapped 95% confidence interval for these estimates are presented in Table 6 to Table 10. Full names of Cohorts are *JHAS*: Johns Hopkins Active Surveillance, *PRIAS*: Prostate Cancer International Active Surveillance, *Toronto*: University of Toronto Active Surveillance, *MSKCC*: Memorial Sloan Kettering Cancer Center Active Surveillance, *KCL*: King's College London Active Surveillance.

Table 7: **External Validation of predictions of Gleason  $\geq 7$  (GS7) in University of Toronto Active Surveillance cohort.** The area under the receiver operating characteristic curve or AUC (measure of discrimination) root mean squared prediction error or RMSPE (measure of calibration) are calculated over the follow-up period at a gap of 6 months. In addition bootstrapped 95% confidence intervals (CI) are also presented.

Follow-up period (years)	AUC (95% CI)	RMSPE (95%CI)
0.0 to 1.0	0.540 [0.493, 0.595]	0.252 [0.236, 0.272]
0.5 to 1.5	0.618 [0.562, 0.660]	0.361 [0.350, 0.373]
1.0 to 2.0	0.653 [0.580, 0.719]	0.405 [0.384, 0.428]
1.5 to 2.5	0.652 [0.596, 0.727]	0.379 [0.358, 0.408]
2.0 to 3.0	0.659 [0.565, 0.743]	0.340 [0.303, 0.369]
2.5 to 3.5	0.606 [0.548, 0.676]	0.368 [0.340, 0.401]
3.0 to 4.0	0.664 [0.583, 0.736]	0.355 [0.324, 0.391]
3.5 to 4.5	0.699 [0.610, 0.773]	0.340 [0.310, 0.374]
4.0 to 5.0	0.617 [0.546, 0.705]	0.397 [0.355, 0.425]

Table 8: **External Validation of predictions of Gleason  $\geq 7$  (GS7) in Johns Hopkins Active Surveillance cohort.** The area under the receiver operating characteristic curve or AUC (measure of discrimination) root mean squared prediction error or RMSPE (measure of calibration) are calculated over the follow-up period at a gap of 6 months. In addition bootstrapped 95% confidence intervals (CI) are also presented.

Follow-up period (years)	AUC (95% CI)	RMSPE (95%CI)
0.0 to 1.0	0.664 [0.604, 0.743]	0.216 [0.198, 0.236]
0.5 to 1.5	0.645 [0.597, 0.695]	0.325 [0.310, 0.339]
1.0 to 2.0	0.661 [0.615, 0.707]	0.320 [0.300, 0.335]
1.5 to 2.5	0.678 [0.587, 0.736]	0.296 [0.277, 0.312]
2.0 to 3.0	0.645 [0.595, 0.701]	0.293 [0.268, 0.317]
2.5 to 3.5	0.558 [0.445, 0.622]	0.281 [0.256, 0.307]
3.0 to 4.0	0.593 [0.498, 0.693]	0.305 [0.281, 0.329]
3.5 to 4.5	0.624 [0.527, 0.690]	0.321 [0.294, 0.340]
4.0 to 5.0	0.593 [0.483, 0.694]	0.329 [0.306, 0.352]

Table 9: **External Validation of predictions of Gleason  $\geq 7$  (GS7) in Memorial Sloan Kettering Cancer Center Active Surveillance cohort.** The area under the receiver operating characteristic curve or AUC (measure of discrimination) root mean squared prediction error or RMSPE (measure of calibration) are calculated over the follow-up period at a gap of 6 months. In addition bootstrapped 95% confidence intervals (CI) are also presented.

Follow-up period (years)	AUC (95% CI)	RMSPE (95%CI)
0.0 to 1.0	0.626 [0.558, 0.681]	0.276 [0.260, 0.297]
0.5 to 1.5	0.605 [0.539, 0.666]	0.340 [0.321, 0.360]
1.0 to 2.0	0.612 [0.564, 0.672]	0.334 [0.316, 0.350]
1.5 to 2.5	0.592 [0.502, 0.670]	0.327 [0.306, 0.345]
2.0 to 3.0	0.638 [0.548, 0.720]	0.332 [0.304, 0.363]
2.5 to 3.5	0.625 [0.542, 0.717]	0.330 [0.303, 0.371]
3.0 to 4.0	0.594 [0.511, 0.655]	0.328 [0.281, 0.368]
3.5 to 4.5	0.599 [0.481, 0.740]	0.350 [0.312, 0.373]
4.0 to 5.0	0.653 [0.562, 0.724]	0.355 [0.320, 0.380]

Table 10: **External Validation of predictions of Gleason  $\geq 7$  (GS7) in King's College London Active Surveillance cohort.** The area under the receiver operating characteristic curve or AUC (measure of discrimination) root mean squared prediction error or RMSPE (measure of calibration) are calculated over the follow-up period at a gap of 6 months. In addition bootstrapped 95% confidence intervals (CI) are also presented.

Follow-up period (years)	AUC (95% CI)	RMSPE (95%CI)
0.0 to 1.0	0.604[0.548, 0.663]	0.389[0.366, 0.411]
0.5 to 1.5	0.676[0.603, 0.744]	0.347[0.328, 0.372]
1.0 to 2.0	0.657[0.578, 0.728]	0.402[0.368, 0.426]
1.5 to 2.5	0.683[0.595, 0.773]	0.438[0.395, 0.469]
2.0 to 3.0	0.664[0.576, 0.735]	0.433[0.396, 0.467]
2.5 to 3.5	0.578[0.443, 0.712]	0.422[0.345, 0.479]
3.0 to 4.0	0.508[0.358, 0.670]	0.380[0.313, 0.452]
3.5 to 4.5	0.566[0.346, 0.776]	0.419[0.354, 0.484]
4.0 to 5.0	0.538[0.295, 0.759]	0.412[0.345, 0.470]

## 127 Appendix C. Personalized Biopsies Based on Risk of GS7

128 Consider some real patients from the PRIAS database shown in Figure 6  
 129 to Figure 9. We intend to develop personalized schedule of biopsies for these  
 130 patients. Using the joint model fitted to the PRIAS dataset, we first ob-  
 131 tain their cumulative risk of GS7 over the entire follow-up period (see Equa-  
 132 tion (4). This cumulative risk accounts for their entire history of PSA as well  
 133 as the time of their latest negative biopsy. For a new patient  $j$  we suggest a  
 134 personalized risk based biopsy if their cumulative risk of GS7  $R_j(s | t, s)$  at  
 135 their current visit  $s$ , given the time of their latest negative biopsy  $t$ , is above  
 136 a certain threshold (e.g., 10% risk). Suppose that in this way a decision of  
 137 biopsy is taken at time  $s$ . Since patients may be removed from AS upon de-  
 138 tection of GS7, subsequent biopsies are scheduled assuming we do not detect  
 139 GS7 at time  $s$ . Thus, at the next visit at time  $s + 1$ , the time of the latest  
 140 negative biopsy is updated to time  $s$ . The updated cumulative risk of GS7  
 141 at time  $s + 1$  is then  $R_j(s + 1 | s, s)$ . If  $R_j(s + 1 | s, s) < 10\%$ , then we decide  
 142 for a biopsy at time  $s + 2$  using the threshold  $R_j(s + 2 | s, s)$ . On the other  
 143 hand if  $R_j(s + 1 | s, s) \geq 10\%$  then then we decide for a biopsy at time  $s + 2$   
 144 using the threshold  $R_j(s + 2 | s + 1, s)$ . While scheduling these biopsies we  
 145 always maintain a minimum gap of one year. Personalized schedules can also  
 146 be made with any other risk threshold such as 5% or 15%.

To assist patients in making an informed choice for a schedule, be it per-  
 sonalized or fixed, we provide them patient-specific consequences of following  
 each schedule. To this end, we first calculate the probability of occurrence of  
 GS7 between successive biopsies of each schedule. Using these probabilities  
 we then obtain the expected delay in detection of GS7 for following that  
 schedule. Thus, patients have a method to compare across various schedules  
 in terms of the personalized burden (time and total biopsies), and personal-  
 ized benefit (less delay in detection of GS7 is beneficial). Suppose once again  
 that for patient  $j$ , the time of latest negative biopsy is  $t$ , and current visit  
 time is  $s > t$ . Then equation for the expected delay  $D_j(\mathcal{S} | t, s)$  in detection  
 of GS7 using schedule of biopsies  $\mathcal{S} = \{t_1, \dots, t_h\}$ , where  $t_1 \geq s$ , and  $t_h$  is  
 the horizon time up to which we want to schedule biopsies, is given by:

$$\begin{aligned}
 D_j(\mathcal{S} | t, s) = & \sum_{v=1}^{h-1} \left\{ R_j(t_{v+1} | t, s) - R_j(t_v | t, s) \right\} \\
 & \times \left\{ t_{v+1} - t_v - \int_{t_v}^{t_{v+1}} \frac{R_j(t_{v+1} | t, s) - R_j(u | t, s)}{R_j(t_{v+1} | t, s) - R_j(t_v | t, s)} du \right\}
 \end{aligned} \tag{5}$$



<sup>147</sup> The personalized and fixed schedules, and their consequences for a few  
<sup>148</sup> real patients from the PRIAS dataset are shown in Figure 6 to Figure 9.

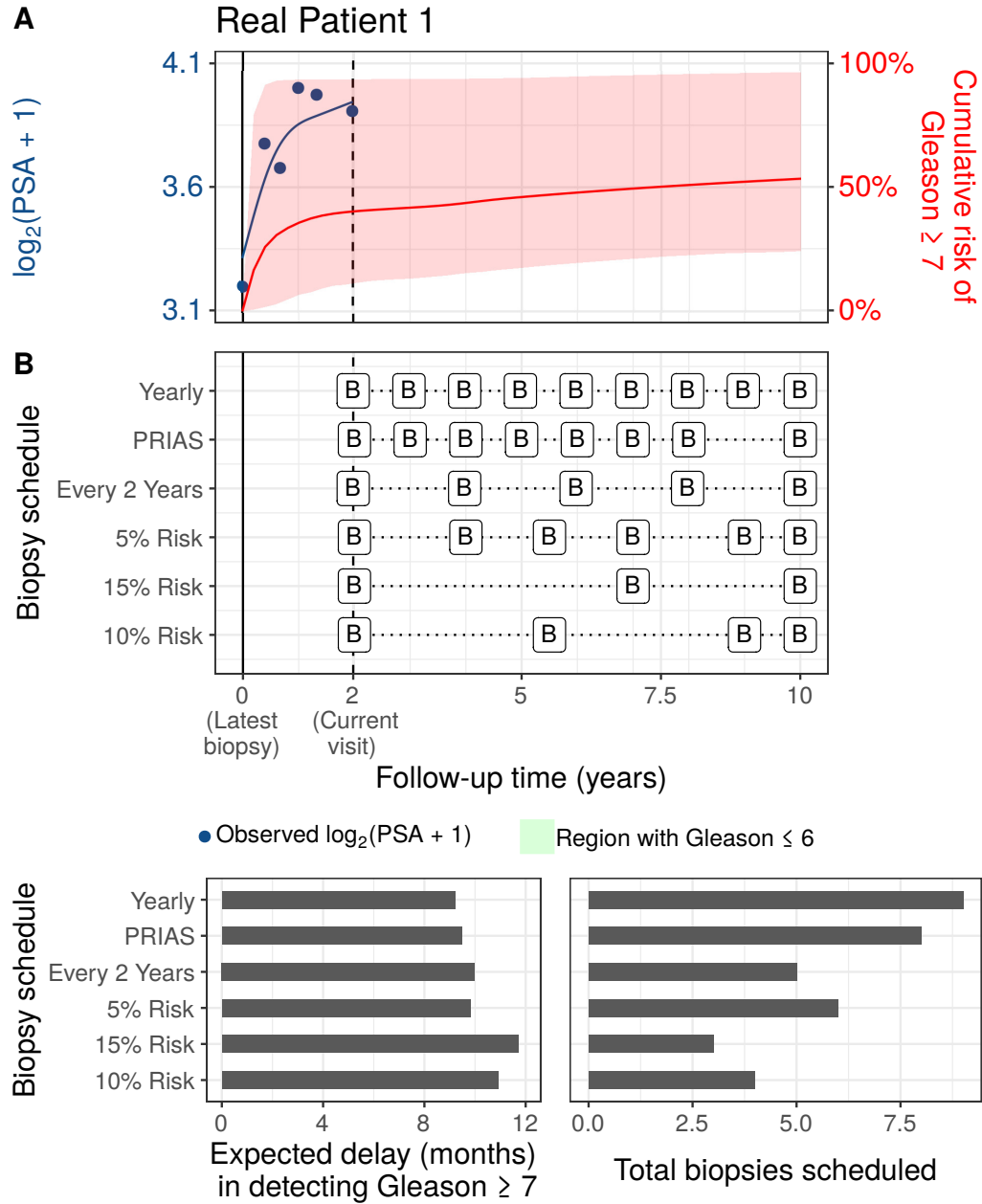


Figure 6: **Personalized and fixed schedules of biopsies patient 1.** **Panel A:** shows the observed and fitted  $\log_2(\text{PSA} + 1)$  measurements (Equation 1), and the dynamic cumulative risk of Gleason  $\geq 7$  (see Appendix B) over follow-up period. **Panel B** shows the personalized and fixed schedules of biopsies with a 'B' indicating times of biopsies. In the bottom two panels, the various schedules are compared in terms of the number of biopsies they schedule, and the expected delay in detection of Gleason  $\geq 7$  if they are followed.

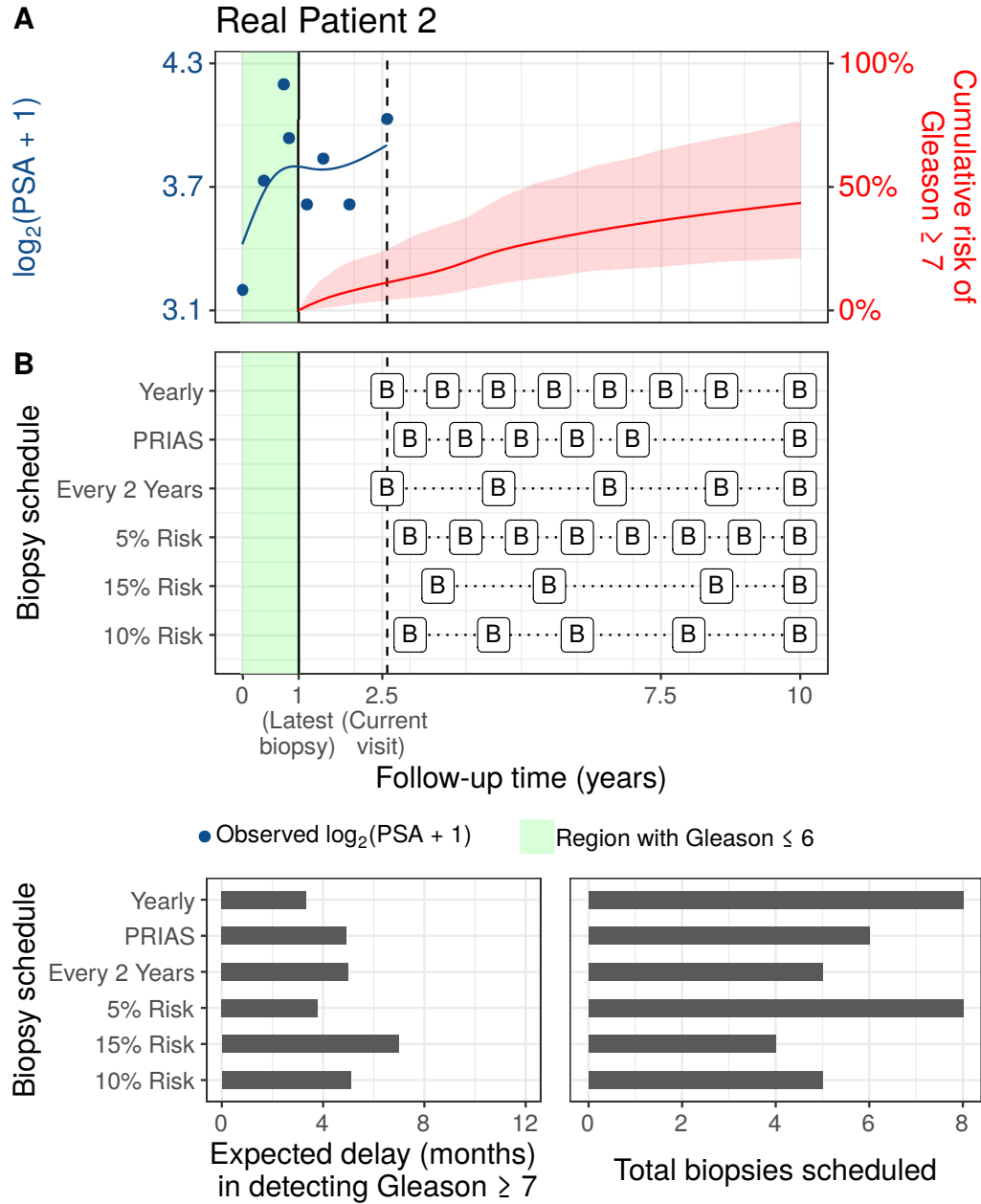


Figure 7: **Personalized and fixed schedules of biopsies patient 2.** **Panel A:** shows the observed and fitted  $\log_2(\text{PSA} + 1)$  measurements (Equation 1), and the dynamic cumulative risk of Gleason  $\geq 7$  (see Appendix B) over follow-up period. **Panel B** shows the personalized and fixed schedules of biopsies with a 'B' indicating times of biopsies. In the bottom two panels, the various schedules are compared in terms of the number of biopsies they schedule, and the expected delay in detection of Gleason  $\geq 7$  if they are followed.

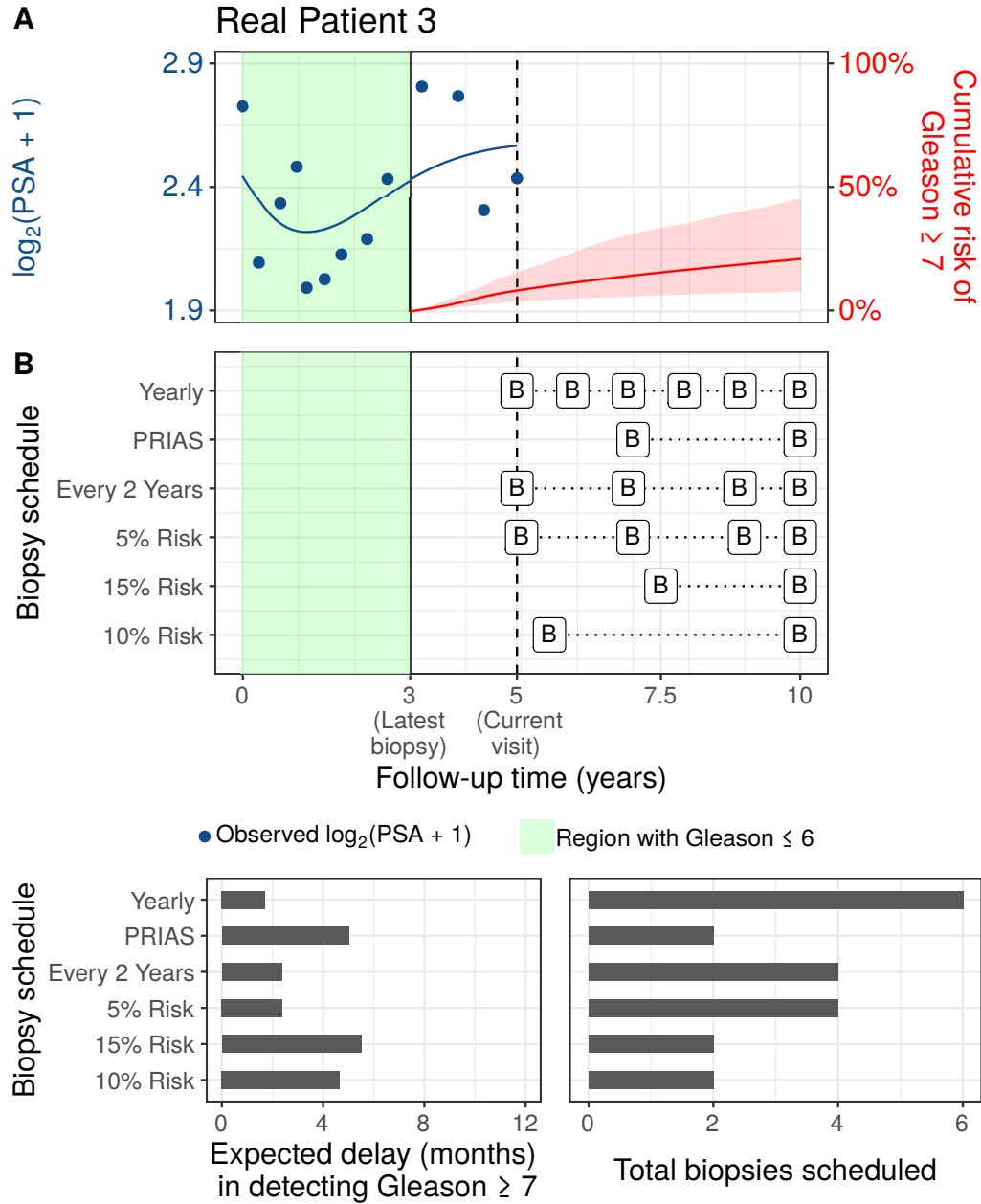


Figure 8: **Personalized and fixed schedules of biopsies patient 3.** **Panel A:** shows the observed and fitted  $\log_2(\text{PSA} + 1)$  measurements (Equation 1), and the dynamic cumulative risk of Gleason  $\geq 7$  (see Appendix B) over follow-up period. **Panel B** shows the personalized and fixed schedules of biopsies with a 'B' indicating times of biopsies. In the bottom two panels, the various schedules are compared in terms of the number of biopsies they schedule, and the expected delay in detection of Gleason  $\geq 7$  if they are followed.

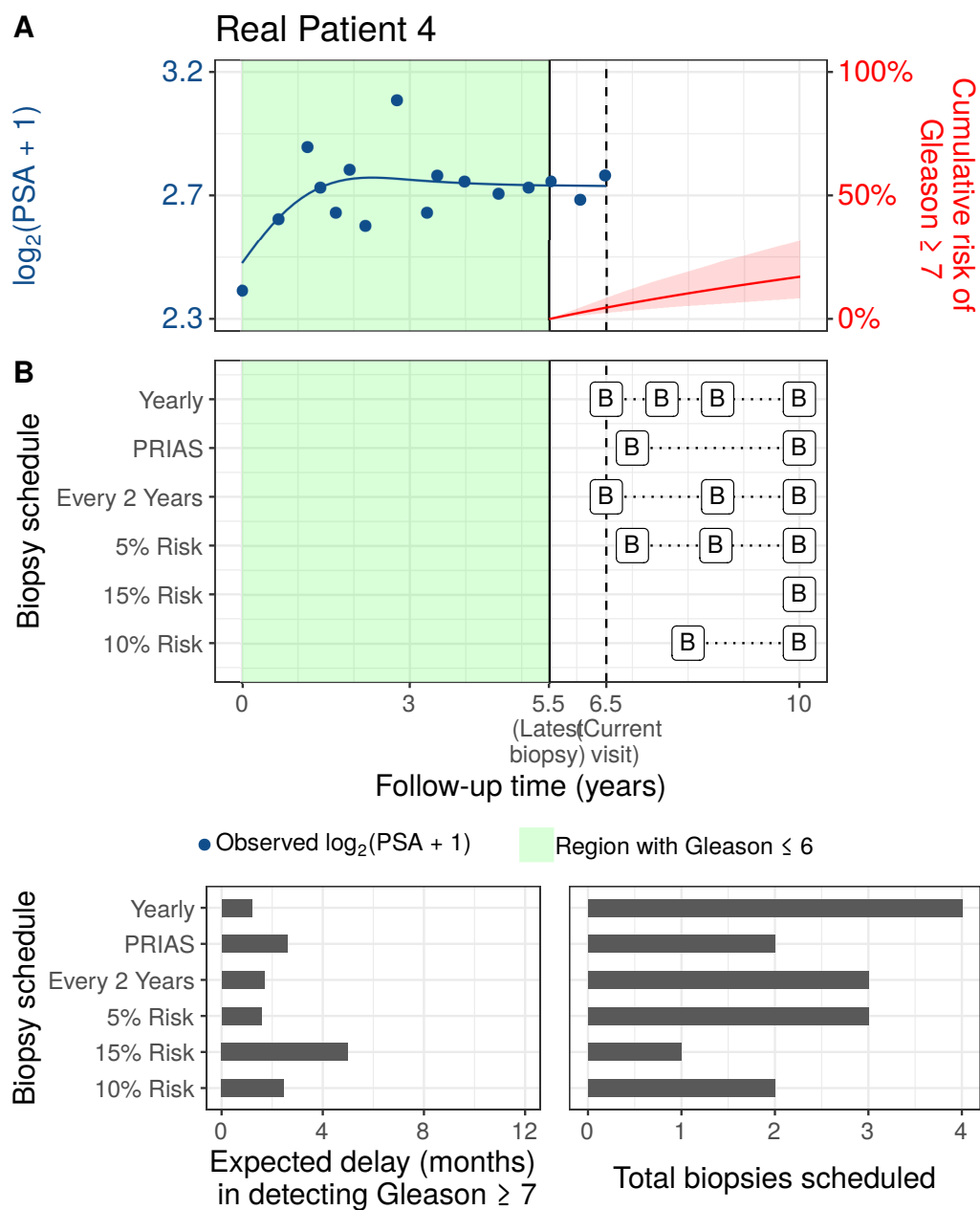


Figure 9: **Personalized and fixed schedules of biopsies patient 4.** **Panel A:** shows the observed and fitted  $\log_2(\text{PSA} + 1)$  measurements (Equation 1), and the dynamic cumulative risk of Gleason  $\geq 7$  (see Appendix B) over follow-up period. **Panel B** shows the personalized and fixed schedules of biopsies with a 'B' indicating times of biopsies. In the bottom two panels, the various schedules are compared in terms of the number of biopsies they schedule, and the expected delay in detection of Gleason  $\geq 7$  if they are followed.

<sup>149</sup> **Appendix D. Web Application for Practical Use of Personalized**  
<sup>150</sup> **Schedule of Biopsies**

## 151 Appendix E. Source Code

152 The R code for fitting the joint model to the PRIAS dataset, is at [https://github.com/anirudhtomer/prias/tree/master/src/clinical\\_gap3](https://github.com/anirudhtomer/prias/tree/master/src/clinical_gap3). We  
 153 refer to this location as ‘R\_HOME’ in the rest of this document.  
 154

### 155 *Appendix E.1. Fitting the Joint Model to the PRIAS dataset*

156 **Accessing the dataset:** The PRIAS dataset is not openly accessible.  
 157 However, access to the database can be requested via the contact links at  
 158 [www.prias-project.org](http://www.prias-project.org).  
 159

160 **Formatting the dataset:** This dataset however is in the so-called  
 161 wide format and also requires removal of incorrect entries. This can be  
 162 done via the R script `R_HOME/dataset_cleaning.R`. This will lead to two  
 163 R objects, namely ‘`prias_final.id`’ and ‘`prias_long_final`’. The ‘`prias_final.id`’  
 164 object contains information about time of GS7 for PRIAS patients. The  
 165 ‘`prias_long_final`’ object contains longitudinal PSA measurements, the time  
 166 of biopsies and results of biopsies.  
 167

168 **Fitting the joint model:** We use a joint model for time to event  
 169 and longitudinal data to model the evolution of PSA measurements over  
 170 time, and to simultaneously model their association with the risk of GS7.  
 171 The R package we use for this purpose is called **JMbayes** (<https://cran.r-project.org/web/packages/JMbayes/JMbayes.pdf>). The API we use, how-  
 172 ever, are currently not hosted on CRAN, and can be found here: <https://github.com/anirudhtomer/JMbayes>. The joint model can be fitted via  
 173 the script `R_HOME/analysis.R`. It takes roughly 6 hours to run on an Intel  
 174 core-i5 machine with 4 cores, and 8GB of RAM.  
 175

176 The graphs presented in the main manuscript, and the supplementary  
 177 material can be generated by the scripts in `R_HOME/plots/`.  
 178

### 179 *Appendix E.2. Validation of Predictions of GS7*

180 Validations can be done using the script `R_HOME/auc_brier/auc_prederr_`  
 181 `no_dre.R`. For external validation access to GAP3 database is required.

### 182 *Appendix E.3. Creating Personalized Schedules of Biopsies*

183 Once a joint model is fitted to the PRIAS dataset, personalized schedules  
 184 of biopsies based on risk of GS7 for new patients can be developed using the

185 script `R_HOME/compareSchedules.R`. This script also provides fixed biopsy  
186 schedules for the patients. In addition with each schedule, the expected delay  
187 in detection of GS7 is also provided.

188 *Appendix E.4. Source Code for Web Application*

189 Source for the shiny web application which provides biopsy schedules for  
190 patients can be found at `R_HOME/shinyapp`



## 191 References

- 192 1. Bul M, Zhu X, Valdagni R, Pickles T, Kakehi Y, Rannikko A, Bjartell  
 193 A, Van Der Schoot DK, Cornel EB, Conti GN, et al. Active surveillance  
 194 for low-risk prostate cancer worldwide: the prias study. *European urology*  
 195 2013;63(4):597–603.
- 196 2. Pearson JD, Morrell CH, Landis PK, Carter HB, Brant LJ. Mixed-effects  
 197 regression models for studying the natural history of prostate disease.  
 198 *Statistics in Medicine* 1994;13(5-7):587–601.
- 199 3. Lin H, McCulloch CE, Turnbull BW, Slate EH, Clark LC. A latent  
 200 class mixed model for analysing biomarker trajectories with irregularly  
 201 scheduled observations. *Statistics in Medicine* 2000;19(10):1303–18.
- 202 4. De Boor C. A practical guide to splines; vol. 27. Springer-Verlag New  
 203 York; 1978.
- 204 5. Eilers PH, Marx BD. Flexible smoothing with B-splines and penalties.  
 205 *Statistical Science* 1996;11(2):89–121.
- 206 6. Rizopoulos D. The R package JMBayes for fitting joint models for lon-  
 207 gitudinal and time-to-event data using MCMC. *Journal of Statistical*  
 208 *Software* 2016;72(7):1–46.
- 209 7. Rizopoulos D, Molenberghs G, Lesaffre EM. Dynamic predictions with  
 210 time-dependent covariates in survival analysis using joint modeling and  
 211 landmarking. *Biometrical Journal* 2017;59(6):1261–76.
- 212 8. Bruinsma SM, Zhang L, Roobol MJ, Bangma CH, Steyerberg EW,  
 213 Nieboer D, Van Hemelrijck M, consortium MFGAPPCASG, Trock B,  
 214 Ehdaie B, et al. The movember foundation’s gap3 cohort: a profile of the  
 215 largest global prostate cancer active surveillance database to date. *BJU*  
 216 *international* 2018;121(5):737–44.